

RSC Advances



This is an *Accepted Manuscript*, which has been through the Royal Society of Chemistry peer review process and has been accepted for publication.

Accepted Manuscripts are published online shortly after acceptance, before technical editing, formatting and proof reading. Using this free service, authors can make their results available to the community, in citable form, before we publish the edited article. This *Accepted Manuscript* will be replaced by the edited, formatted and paginated article as soon as this is available.

You can find more information about *Accepted Manuscripts* in the [Information for Authors](#).

Please note that technical editing may introduce minor changes to the text and/or graphics, which may alter content. The journal's standard [Terms & Conditions](#) and the [Ethical guidelines](#) still apply. In no event shall the Royal Society of Chemistry be held responsible for any errors or omissions in this *Accepted Manuscript* or any consequences arising from the use of any information it contains.

23 **Abstract:**

24 Peroxynitrous acid (ONOOH) produced by online mixing of nitrite and acidified hydrogen
25 peroxide could induce weak chemiluminescence (CL). A stronger chemiluminescence was
26 observed in the presence of gold nanoclusters (Au NCs). This novel CL system was
27 developed as a flow-injection method for the nitrite determination directly and conveniently.
28 This method was achieved in acidic medium, which greatly improve its selectivity. The CL
29 mechanism of the peroxynitrous acid-gold nanoclusters system was investigated using the
30 CL spectra, UV-visible spectroscopy and radical scavengers. The enhanced CL could be
31 attributed to the catalysis of Au nanoclusters. The proposed method has been applied to
32 determine nitrite in water samples with good accuracy and precision.

33

34 **Keywords:**

35 Gold nanoclusters; flow-injection; chemiluminescence; peroxynitrous acid; nitrite.

36

37

38

39

40

41

42

43

44

45 **1. Introduction**

46 Nitrite, as a characteristic pollutant and fertilizing agent for food, is widely present in the
47 environment [1, 2]. The reaction of nitrite with secondary amines could form carcinogenic
48 N-nitrosamines, which is extremely harmful to humankind [3]. Thus, the concentration of
49 nitrite in water environment is one of the most important indicators of water quality. It is
50 also reported that nitrite has caused serious hazards to the nervous system, spleen and
51 kidneys. Therefore, it is of great importance to detect nitrite quantitatively in water sources.

52 Due to the harmness of nitrite to environment and human health, a lot of analytical
53 methods based on different principles have been developed for the determination of nitrite,
54 such as UV-vis absorbance[4,5], electrochemistry[6,7], chemiluminescence (CL)
55 [8-10,15-20] and fluorometric approaches[11-13]. The conventional UV-vis absorbance
56 methods for determinatng nitrite are usually based on the diazo coupling reaction [4, 5]. In
57 order to obtain high sensitivity and selectivity, the long coupling process requires exquisite
58 control of pH and temperature. The electrochemical process always needs complex
59 electrodes [6, 7]. Fluorescent dyes are necessary for the fluorescent detection, which need
60 to react with nitrite in this process, thus may cause potential strong background
61 fluorescence in the real samples [13].

62 Chemiluminescence, as a sensitive, facile, and rapid analytical method, has been well
63 applied to the detection of nitrite in environmental monitoring and food safety. The gas
64 phase CL assays for nitrite [8, 14] are based on the reduction of nitrite to nitric oxide (NO),
65 which could react with ozone to produce CL signal. However, such transformation suffers
66 from complicated procedure. In the aqueous phase [15], the detection of nitrite is based on

67 that nitrite can react with acidified hydrogen peroxide to form unstable peroxyntrous acid
68 (ONOOH), which can be quenched to peroxyntrite by an alkaline reagent. The
69 decomposition of peroxyntrite with weak CL signal has been developed as a flow-injection
70 method for nitrite sensing [16]. Mikuska et al. [17] reported peroxyntrous acid (ONOOH)
71 can react with alkaline luminol and built a CL method for the nitrite detection. The weak
72 CL from excited peroxyntrous acid also could be amplified by energy acceptors, such as
73 uranine [16], CdTe quantum dots [18], Fluorosurfactant (FSN)-gold nanoparticles [19].
74 These methods were interfered with some transition metals, because they were achieved in
75 alkaline media. In order to improve the selectivity, cation-exchange column was introduced,
76 which may make the detection more complex. Therefore, it is an attractive research area to
77 develop more simple and convenient ONOOH/ONOO⁻ CL reactions in acidic system.

78 As a new class of metal nanostructures, metal nanoclusters (NCs) have attracted great
79 attention due to their unique properties and versatile applications [20-26]. Among the metal
80 nanoclusters, Au nanoclusters (Au NCs) exhibit fascinating features, including facile
81 synthesis, good water solubility, low toxicity, and long term stability. Because of these
82 attractive features, gold nanoclusters have attracted significant research efforts recently.
83 Until now, the application of Au NCs in analytical fields mainly focused on their
84 fluorescence properties. It would be interesting to find that AuNCs have effect on peroxide
85 induced ultra-weak CL reactions. In this work, we found that the weak CL emission from
86 the reaction of nitrite with hydrogen peroxide in acidic medium was greatly enhanced by
87 Au NCs. And the CL intensity was proportional to the concentration of nitrite, which led to
88 a novel sensing platform based on the activities of Au NCs in direct nitrite determination.

89 The proposed method was achieved in acidic medium, which greatly improve its selectivity.
90 This method can be used to detect trace nitrite in tap water, river water and pond water with
91 acceptable selectivity and reproducibility. This work is an example of the successful
92 analytical application of nanoparticles-enhanced CL.

93

94 **2. Experimental**

95 *2.1 Reagents and materials.*

96 All chemical reagents were of analytical grade and used without further purification.
97 And ultrapure water was used throughout. Sodium nitrite was obtained from Chongqing
98 Beibei Chemical Reagent Co. Ltd. (Chongqing, China). $\text{HAuCl}_4 \cdot 3\text{H}_2\text{O}$ was purchased
99 from Sinopharm Chemical Reagent Co. Ltd. (Shanghai, China). Bovine serum albumin
100 (BSA) was supplied by Sangon Biotech Co. Ltd. (Shanghai, China). Hydrogen peroxide
101 (H_2O_2 , 30%), sodium hydroxide, Sulfuric acid (98%) and nitro blue tetrazolium (NBT)
102 were purchased from Kelong Reagent Co. Ltd. (Chengdu, China). Thiourea and ascorbic
103 acid (AA) were commercially obtained from Chongqing Chemical Regent Company
104 (Chongqing, China).

105

106 *2.2 Synthesis of BSA-Au nanoclusters.*

107 BSA stabilized Au NCs were synthesized in aqueous solution according to the
108 previously reported method [27]. In a typical experiment, all the glassware were
109 thoroughly cleaned with aqua regia ($V_{\text{HNO}_3} : V_{\text{HCl}}$, 1:3) and rinsed extensively with double
110 distilled water prior to use. Aqueous HAuCl_4 solution (5 mL, 10 mM, 37 °C) was added

111 to BSA solution (5 mL, 50 mg/mL, 37 °C) under vigorous stirring. Two minutes later, an
112 aqueous solution of NaOH (0.5 mL, 1 M) was introduced, and the mixture was incubated
113 at 37 °C for 24 h under vigorous stirring. The color of the solution changed from light
114 yellow to light brown, and then to deep brown. The solution was then dialyzed in
115 ultra-pure water for 24 h to remove unreacted BSA. The final solution was stored at 4°C
116 in refrigerator when not in use.

117

118 *2.3 Sample preparation.*

119 Tap water was analyzed without any pretreatment. River water and pond water were
120 filtered through a membrane filter of 0.22-µm pore size and spiked with 1.0×10^{-5} M
121 EDTA as a masking reagent for transition metal before the CL determination.

122

123 *2.4 General procedure for CL analysis.*

124 The FI system, as shown in Fig.1, was carried out on a laboratory-built flow injection
125 CL system (Xi'an Remax Company, Xi'an, China) . The flow-injection system was
126 consisted of two peristaltic pumps to deliver the reactants to the flow cell. One delivered
127 water (Water was used as the carrier for nitrite and sample.) with one channel at a flow
128 rate (per tube) of 2.0 mL/min. The other pump was used to carry H₂O₂ and Au NCs
129 solution with two channels at the same flow rate. The PTFE tubing (0.8 mm i.d.) was used
130 to connect all components in the flow system. A six-way injection valve equipped with an
131 8 cm long sampling loop was used to inject. The CL signal was detected by a
132 photomultiplier tube (operated at -1k V), and then recorded by a computer equipped with

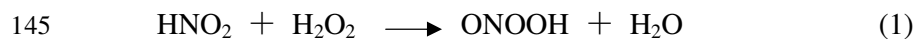
133 a data acquisition interface. Data acquisition and treatment were performed with BPCL
134 software running under Windows XP. Determination of nitrites was performed based on
135 the net CL intensity of $\Delta I = I_0 - I_s$, where I_0 and I_s denote the CL intensity in the absence
136 and presence of nitrites, respectively.

137

138 **3. Results and discussion**

139 *3.1 CL from Au NCs-NaNO₂-H₂O₂ system.*

140 ONOOH, as a small inorganic nitrogen-containing hydroperoxide, is a strong acid. A
141 method for preparation of ONOOH is the reaction of NaNO₂ with H₂O₂ in acid medium
142 [28]. In this work, ONOOH was formed by the online mixing of NaNO₂ and acidified H₂O₂
143 (Reaction 1) [39-30]. Then, light emission was caused from the transform of ONOOH to
144 nitrite via the stage of HOONO* (Reaction 2) [32-33].



147 The ultra-weak CL emission resulting from the reaction of NaNO₂ and acidified H₂O₂
148 was recorded in Fig.2 (A) curve 1. However, the interaction mentioned was accompanied
149 by a strong CL signal in the presence of Au NCs (curve 2). From it, we can see the CL
150 signal intensity was enhanced about 20 times when the Au NCs was introduced. As shown
151 in Fig.2 (B), the reaction between Au NCs and H₂O₂ brought a weak CL enhancement in
152 comparison of two CL signal curves, which indicated that the contribution of H₂O₂ to the
153 high CL intensity could not be ignored. From the above CL signals, we believe that the

154 system of Au NCs-NaNO₂-H₂O₂ can be developed as a flow-injection analysis for the
155 detection of nitrite.

156

157 *3.2 Optimization of the reaction conditions.*

158 To establish the optimal conditions for the analysis of nitrite, the effects of the
159 concentration of H₂SO₄, Au NCs, H₂O₂ and flow rate on the CL analysis were investigated
160 (Fig.3). It was found that no CL signal has been discovered in the absence of H₂SO₄,
161 because ONOOH only could be formed in an acidic medium. Therefore, the concentration
162 of H₂SO₄ was investigated in the range of 0.01-0.5 M (Fig.3A). With the increase of
163 concentration from 0.01 to 0.04 M, the CL intensity increased sharply and then decreased
164 obviously beyond 0.3 M. As a consequence, 0.04 M was selected as the optimum H₂SO₄
165 concentration in the present system.

166 The effect of H₂O₂ concentration on the CL was studied in the range from 0.01 to 0.05 M
167 (Fig. 3B), the CL intensity increased with the increasing H₂O₂ concentration in the range of
168 0.01 to 0.2 M and changed slowly beyond 0.3 M. Consequently, 0.2 M was chosen as the
169 optimal H₂O₂ concentration in the present study.

170 The flow rate was discussed as shown in Fig. 3D. We found that the CL signal increased
171 with the increasing flow rate. As we all know, a slower or more rapid flow rate could lead to
172 a CL reaction occurring before or behind the flow cell. Thus, 2.0 mL/min was chosen as the
173 most suitable flow rate. The effect of the concentration of Au NCs was also investigated in
174 the range of 2.0×10⁻⁶ to 6.0×10⁻⁵ M, and the optimal concentration was 8.0×10⁻⁶ M (Fig.3C).

175 In view of the CL intensity and the consumption of the reagents, the optimized conditions

176 for CL system were as follows: 0.2 M H₂O₂ in H₂SO₄ solution (0.04 M), 8.0× 10⁻⁶ M Au
177 NCs, and the flow rate was 2.0 mL/min.

178

179 *3.3 Mechanism Discussion.*

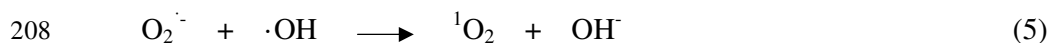
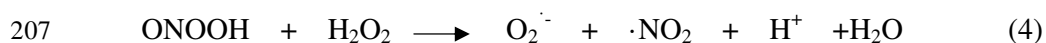
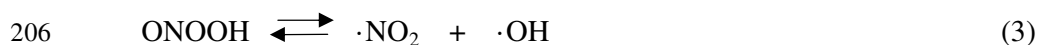
180 The ultra-weak CL emission resulting from the reaction of NaNO₂ and acidified H₂O₂
181 was owing to the transform of ONOOH to nitrite via the stage of HOONO*. It was found
182 the effect of nanoparticles in a liquid-phase CL reaction could act as catalysts [31] or
183 emitters [32]. A F-2500 mode fluorescence spectrophotometer with the xenon lamp turned
184 off had been used to discuss the CL mechanism of NaNO₂-H₂O₂ system in the presence or
185 absence of Au NCs. As shown in Fig.4, the CL spectrum for Au NCs-NaNO₂-H₂O₂ system
186 located in the range of 360-400 nm and centered at 379 nm. While the light emission from
187 the transform of ONOOH to nitrate via the HOONO* stage is believed in the wavelength
188 region of 350-450 nm [33-34], which is in good agreement with the CL spectrum of Au
189 NCs-NaNO₂-H₂O₂ system. Therefore, the adding of Au NCs did not generate a new
190 luminophor in this CL system. The enhanced CL signal was thus attributed to the possible
191 catalysis from Au NCs.

192 In order to further confirm the possible mechanism, the UV-visible absorption spectra
193 were recorded. As shown in Fig. 5, the maximum absorption peak of NaNO₂ was observed
194 at around 354 nm. The peak became lower with the addition of acidified H₂O₂ into NaNO₂
195 solution. This change could be attributed to the isomerization of ONOOH, which was
196 formed by the mixing of NaNO₂ and acidified H₂O₂ (Reaction 2). No new absorption peak
197 appeared when Au NCs were introduced into NaNO₂-H₂O₂ system. From the above all, the

198 enhancement of CL signal might be derived from the catalytic effect of Au NCs.

199 The mechanism was also confirmed by the quenching effect of different reactive oxygen
200 species (ROS) on the CL system. Singlet oxygen ($^1\text{O}_2$) as a CL emitter has been reported to
201 exist in the $\text{NaNO}_2\text{-H}_2\text{O}_2$ system (Reaction 3-5) [35]. Sodium azide (NaN_3), a well-known
202 quencher of singlet oxygen ($^1\text{O}_2$) [35, 36], was used in the present experiment. And the result
203 showed that 5 mM NaN_3 had no inhibition of the CL intensity, which provided strong
204 evidence that $^1\text{O}_2$ was not existing in the Au NCs- $\text{NaNO}_2\text{-H}_2\text{O}_2$ system. (Table.1)

205



209

210 Ascorbic acid (AA) is well known as an efficient ROS scavenger [37], it can terminate
211 active oxygen radicals by electron transfer. Ascorbic acid with a concentration of 1 mM had
212 a negative effect on the signal, which illustrated that the generation of free radicals
213 appeared to be important in the CL reaction. NBT is frequently used for the detection of
214 $\text{O}_2^{\cdot-}$ radicals, because it can reduce NBT to its deep blue diformazan form [38]. When 1mM
215 NBT was added to the CL system, the CL intensity decreased by a factor of ~60.0.
216 Thiourea is an effective radical scavenger for hydroxyl radical ($\text{OH}\cdot$) [39]. When 5 mM
217 thiourea was added to the CL system, a distinct inhibition was observed by the factor of
218 ~61.1. The results evidently supported the assumption that $\text{O}_2^{\cdot-}$ and $\text{OH}\cdot$ was the
219 intermediate in the CL reaction. It was reported that H_2O_2 decomposition on supported

220 metal catalysts such as Au NPs, Ag NPs and CuO NPs involved the formation of hydroxyl
221 radicals $\text{OH}\cdot$. We suggested that the O–O bond of H_2O_2 might be broken up into double
222 $\text{OH}\cdot$ radicals by virtue of the catalysis of Au nanoclusters. Then the $\text{OH}\cdot$ radicals reacted
223 with $\cdot\text{NO}_2$ to form the ONOOH (Reaction 3), and then ONOOH was transformed to nitrate
224 via the HOONO^* , which cause the light emission. Based on the above results, the whole
225 enhanced mechanism is summarized in Scheme.1.

226

227 *3.4 Analytical performance.*

228 Nitrite is widely present in the environment and is used as preservatives and fertilizing
229 reagents for food. The possibility of proposed method to detect nitrite was studied (Fig. 6).
230 Under the optimum conditions described above, there is a good linear relationship between
231 CL intensity and the nitrite concentration in the range from 5 μM to 0.1 mM with a
232 correlation coefficient of 0.9991 and the regression equation is $\Delta I = 24.05 + 48.46 [\text{Nitrite}]$
233 (M). The limit of detection (LOD, 3σ) for nitrite was 4.7 μM . The relative standard
234 deviation (RSD) for 9 repeated measurements of 0.8 μM nitrite was 2.3%.

235

236 *3.5 Interference study.*

237 The selectivity of the proposed method was evaluated by analyzing a standard solution
238 of 6×10^{-5} M nitrite, to which varying amounts of possible interferences were added. The
239 tolerance limit was taken as the amount which caused an error of less than 5% for the
240 determination of 6×10^{-5} M nitrite. The results were summarized in Fig.7. Most of the
241 interferences have no influence on the determination of nitrite, because the acidic medium

242 could highly reduce the interference from the transition metals. Therefore, the results
243 indicated that the proposed CL system is highly selective for nitrite.

244

245 *3.6 Analytical applications.*

246 In order to evaluate the applicability and reliability of the proposed method, it was
247 applied to the determination of nitrite in real samples, such as tap water, pond water, and
248 river water. From Table.2, it can be seen that the recovery of nitrite in real samples ranged
249 from 95.5 to 110.2% through standard addition experiments, which demonstrated the
250 proposed CL system was satisfactory for nitrite analysis. Meanwhile, the analytical results
251 of the proposed method were evaluated by the national food safety standard (GB
252 5009.33-2010) [40]. As shown in Table.3, the results that obtained with the two methods
253 were in accordance with the sample determination.

254

255 **4. Conclusion**

256 In summary, gold nanoclusters were first demonstrated as a catalyst in the ultra-weak CL
257 system of peroxyxynitrous acid, which was formed by the online reaction of acidified H_2O_2 and
258 NaNO_2 . The acidic medium also could highly reduce the interference from the transition
259 metals. The enhanced CL could be attributed to the catalysis of Au nanoclusters, which
260 effectively catalyzed the decomposition of H_2O_2 to produce double hydroxyl radicals. With
261 the advantage of the CL of ONOOH in the presence of gold nanoclusters, we have developed
262 a sensitive, simple, and straightforward flow-injection CL method for nitrite determination.
263 The established method has been successfully applied to the determination of nitrite in pond

264 water, tap water, and river water with good recovery and high reproducibility.

265

266 **Acknowledgements**

267 This work was supported by science and technology commission foundation of Chongqing

268 (CSTC, 2010BB8328)

269 We thank Prof. H. Z. Zheng and Prof. Y. M. Huang for measurements.

270

271

272

273

274

275

276

277

278

279

280

281

282

283

284

285

286 **Figure captions**

287 **Scheme.1.** Possible mechanism for the Au NCs-NaNO₂-H₂O₂ system.

288

289 **Fig.1.** Schematic diagram of the flow-injection manifolds for Au NCs-NaNO₂-H₂O₂
290 detection system. P1, P2 stand for two peristaltic pumps for solution delivery. R1: H₂O as
291 the carrier; R2: Au NCs; R3: H₂O₂.

292

293 **Fig.2.** A: CL kinetic curves of NaNO₂-H₂O₂ system (curve 1) and Au NCs-NaNO₂-H₂O₂
294 system (curve 2). B: CL kinetic of H₂O₂ and the Au NCs-H₂O₂ system. Experimental
295 condition: 0.2 M H₂O₂ in 0.04 M H₂SO₄, 8.0×10⁻⁶ M Au NCs, flow rate was set as 2.0
296 mL/min.

297

298 **Fig.3.** Effect of (A) the concentration of H₂SO₄, (B) the concentration of H₂O₂ (C) the
299 concentration of Au NCs (D) the flow rate on the flow-injection CL detection system.

300

301 **Fig. 4.** CL spectrum of the Au NCs-NaNO₂-H₂O₂ system. (Experiment conditions: the PMT
302 voltage was set at 700V, and the slit width of excitation and emission was 5 nm.)

303

304 **Fig.5.** UV-vis absorption of the reagent in the CL reaction. Experimental condition: 0.2 M
305 H₂O₂ in 0.04 M H₂SO₄, 8.0×10⁻⁶ M Au NCs, 6.0×10⁻⁵ M nitrite, flow rate was set as 2.0
306 mL/min.

307

308 **Fig.6.** Standard curve for the nitrite concentration in the range from 5×10⁻⁶-1×10⁻⁴ M.

309 Experimental condition: 0.2 M H₂O₂ in 0.04 M H₂SO₄, 8.0×10⁻⁶ M Au NCs, 6.0×10⁻⁵ M
 310 nitrite, flow rate was 2.0 mL/min.

311

312 **Fig.7** Selectivity for nitrite assay against some interfering species with respect to 6.0×10⁻⁵
 313 M nitrite. The concentration of some species (NO₃⁻, Na⁺, SO₄²⁻, Cl⁻, CO₃²⁻, H₂PO₄⁻, HPO₄²⁻,
 314 K⁺, Mg²⁺, F⁻ and glucose) was 10 mM; 1 mM for Ca²⁺, Zn²⁺ and NH₄⁺; 0.1 mM for Fe³⁺,
 315 Cu²⁺, malic acid and citric acid; 0.01 mM for Γ. Experimental condition: 0.2 M H₂O₂ in
 316 0.04 M H₂SO₄, 8.0×10⁻⁶ M Au NCs, flow rate was set as 2.0 mL/min.

317

318 **Tables:**

319 **Table.1** Effect of different radical scavengers on the CL of nitrite-H₂O₂ in the presence of
 320 Au nanoclusters^a

Scavengers	Intermediates	Concentration	Percent inhibition ^b (%)
H ₂ O			0
NaN ₃	¹ O ₂	5mM	6
Ascorbic acid	OH [·] , O ₂ ^{·-}	1mM	26.5
NBT	O ₂ ^{·-}	1mM	60.0
Thiourea	OH [·]	5mM	61.1

321

322 ^aSolution condition: 0.2 M H₂O₂ in 0.04 M H₂SO₄, 8.0×10⁻⁶ M AuNCs, 6×10⁻⁵ M nitrite.

323 ^bAverage value of three determination.

324

325

326

327

328 **Table 2** Result of recovery test on nitrite determination (n =3) for water samples.

329

Samples	Added (10^{-5} M)	Found (10^{-5} M)	Recovery (%)
Tap water	2	1.91±0.01	95.5
	3	3.16±0.04	105.3
	8	8.01±0.01	100.1
Pond water	6	6.04±0.04	100.6
	8	7.67±0.03	95.9
	9	8.99±0.01	99.9
River water	2	2.03±0.03	101.5
	4	4.41±0.01	110.2
	6	5.90±0.02	98.3

330

331

332

333 **Table 3** Determination of nitrite in water samples (n=3).

334

Samples	Proposed method	spectrophotometric
	Nitrite(10^{-5} M)	method ^a (10^{-5} M)
Tap water	1.91±0.01	1.96±0.02
Pond water	6.04±0.04	6.10±0.02
River water	2.03±0.03	1.97±0.02

335 ^aData taken from ref 34.

336

337

338

339

340

341

342 **References**

- 343 [1] I. A. Wolff and A.E. Wasserman, *Science*.**1972**, *177*, 15-19.
- 344 [2] K. K. Choi and K. W. Fung, *Analyst*. **1980**,*105*, 241-245.
- 345 [3] M. Masuda, H.F. Mower, B. Pignatelli, I. Celan, M.D. Friesen,H. Nishino and H.
- 346 Ohshima, *Chem. Res. Toxicol.* **2000**, *13*, 301-308.
- 347 [4] Afkhami. A, Bahram. M, Gholami. S, Zand, *Z.Anal. Biochem.* **2005**, *336*, 295–299.
- 348 [5] Muscara. M. N, Nucci. G. D, *J. Chromatogr. B.* **1996**, *686*, 157–164.
- 349 [6] R. Geng, G. H. Zhao, M. C. Liu, M. F. Li. *Biomaterials.* **2008**, *29*, 2794–280.
- 350 [7] J. Davis, M. J. Moorcroft, S. J. Wilkins, R. G. Compton, M. F. Cardosi. *Analyst*, **2000**,
- 351 *125*, 737–742.
- 352 [8] R.D. Cox, *Anal. Chem.* **1980**, *52*, 332–335.
- 353 [9] J.E. Li, Q.Q. Li, C. Lu and L.X. Zhao, *Analyst.* **2011**, *136*, 2379–2384.
- 354 [10] Z. Lin, W. Xue, H. Chen and J.M. Lin, *Anal. Chem.* **2011**, *83*, 8245–8251.
- 355 [11] D.W. Bedwell, V.R. Rivera, G.A. Merrill and A.E. Pusaterr, *Anal.Biochem.* **2000**, *284*,
- 356 *1-5*.
- 357 [12] N. Jie, J. Yang and J. Li, *Anal. Lett.* **1994**, *27*, 1001-1005.
- 358 [13] X.Q. Zhan, D.H. Li, H. Zheng and J.G. Xu, *Anal. Lett.* **2001**, *34*, 2761-2770.
- 359 [14] A.R. Thornton, J. Pfab and R.C. Massey, *Analyst.* **1989**,*114*, 747-748.
- 360 [15] Berckman. J. S, Beckman. T. W, Chen. J, Marshall. P, Freeman. B. A. *Proc. Nati. Acad.*
- 361 *Sci. U.S.A.* **1990**, *87*, 1620–1624.
- 362 [16] Lu.C, Qu. F, Lin. J.M and Yamada. M, *Anal. Chim. Acta.* **2002**,*474*, 107–114.
- 363 [17] P. Mikuska, Z. Vecera and Z. Zdrahal, *Anal. Chim. Acta.* **1995**,*316*, 261-268.

- 364 [18] H.X. Zhang, L. J. Zhang, C. Lu, L. X. Zhao, Z. X. Zheng, *Spectrochimica Acta Part*
365 *A* .**2012**,*85*, 217–222.
- 366 [19] J. G. Li, Q. Q. Li, C. Lu , L.X. Zhao. *Analyst*, **2011**,*136*, 2379–2384.
- 367 [20] G. Sivaraman, T. Anand and D. Chellappa, *Analyst*. **2012**, *137*, 5881-5884.
- 368 [21] V.Tharmaraj, S.Devi and K. Pitchumani, *Analyst*. *2012*, *137*, 5320-5324.
- 369 [22] J. Zheng, C. Zhou, M. Yu and J. Liu, *Nanoscale*. **2012**, *4*, 4073–4083.
- 370 [23] L. Shang, S. Dong and G. U. Nienhaus, *Nano. Today*. **2011**, *6*, 401–418.
- 371 [24] H. Xu, K. S. Suslick, *Adv. Mater*, **2010**, *22*, 1078–1082.
- 372 [25] R. Jin, *Nanoscale*. **2010**, *2*, 343–362.
- 373 [26] W. Wei, Y. Lu, W. Chen and S. Chen, *J. Am. Chem. Soc.* **2011**, *133*, 2060–2203.
- 374 [27] J. P. Xie, Y. G. Zheng, Jackie Y. Ying, *J. Am. Chem. Soc.* **2009**,*131*, 888–889.
- 375 [28] Z. Lin, H. Chen and J. M. Lin, *Analyst*. **2013**, *138*, 5182-5193.
- 376 [29] S. Ahmed, N. Kishikawa, K. Ohyama, T. Maki, H. Kurosaki, K. Nakashima and N.
377 Kuroda, *J. Chromatogr. A*. **2009**, *1216*, 3977–3984.
- 378 [30] Anbar. M, Taube. H, *J. Am. Chem. Soc.* **1954**, *76*, 6243–6247.
- 379 [31] Zhang.Z.F, Cui.H, Lai.C.Z and Liu.L.J, *Anal. Chem.* **2005**, *77*, 3324–3329.
- 380 [32] Chen. H, Lin. L, Lin. Z, Guo. G. S, Lin. J.M, *J. Phys.Chem. A*. **2010**,*114*, 10049–10058.
- 381 [33] Starodubtseva. M. N, Cherenkevich. S. N, Semenkova. G. N, *J. Appl. Spectrosc.* **1999**,
382 *66*, 473–476
- 383 [34] Houk. K. N, Condroski. K. R and Pryor. W. A, *J. Am. Chem. Soc.* **1999**, *118*,
384 13002–13006.
- 385 [35] Hosaka. S, Itagaki. T, Kuramitsu. Y, *Luminescence*, **1999**, *14*,349–354.

- 386 [36] Lin. J.M, Yamada. M, *Anal. Chem.* **2000**, *72*, 1148–1155.
- 387 [37] Dai. H, Wu. X. P, Wang. Y. M, Zhou. W. C, Chen. G. N, *Electrochim. Acta* , **2008**, *53*,
- 388 5113–5117.
- 389 [38]Bielski. B. H. J, Shiue. G. G, Bajuk. S, *J. Phys. Chem.* **1980**, *84*,830–833.
- 390 [39] Wang. W. F, Schuchmann. M. N, Schuchmann. H. P, Knolle.W, Sonntag. J. V, Sonntag.
- 391 C. V, *J. Am. Chem. Soc.* **1999**, *121*, 238–245.
- 392 [40] Sreekumar. N. V, Narayana. B, Hegde. P, Manjunatha. B. R and Sarojini. B. K,
- 393 *Microchem. J.* **2003**, *74*, 27–32.

Figures content:

1. Fig.1
2. Fig.2 (A)
3. Fig.2 (B)
4. Fig.3 (A)
5. Fig.3 (B)
6. Fig.3 (C)
7. Fig.3 (D)
8. Fig.4
9. Fig.5
10. Scheme.1
11. Fig.6
12. Fig.7

Fig.1

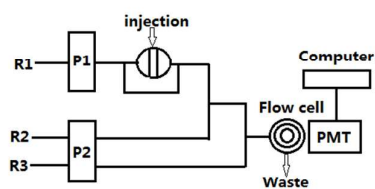


Fig.2(A)

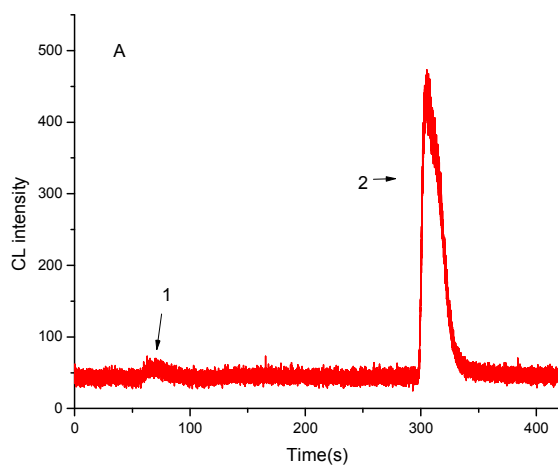


Fig.2(B)

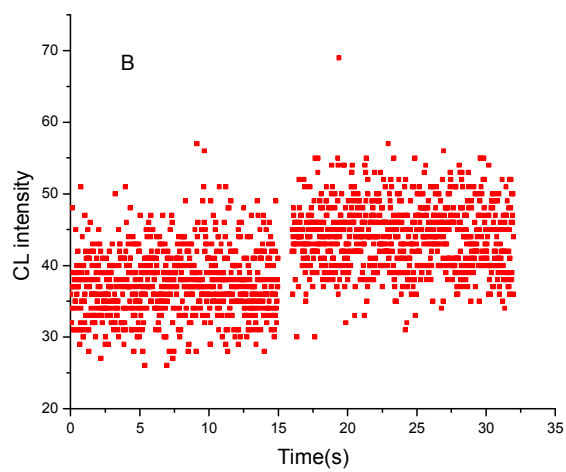


Fig.3(A)

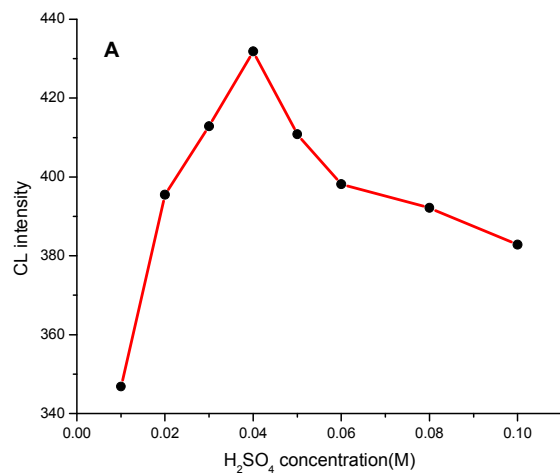


Fig.3(B)

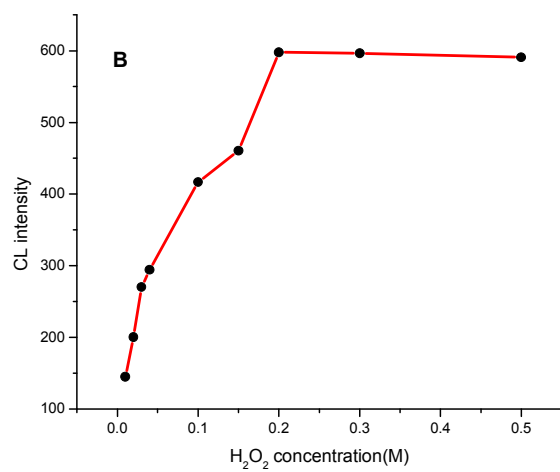


Fig.3(C)

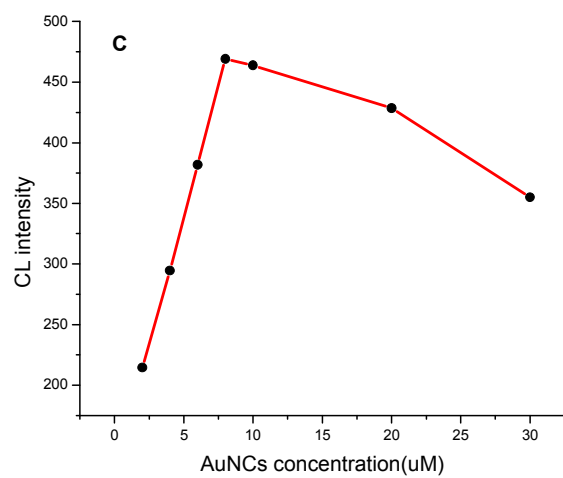


Fig.3(D)

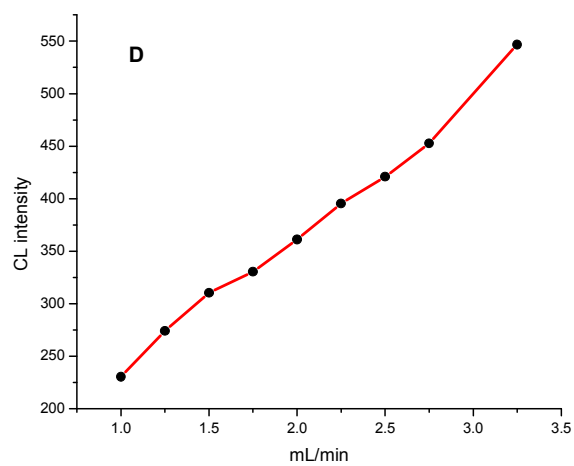


Fig.4

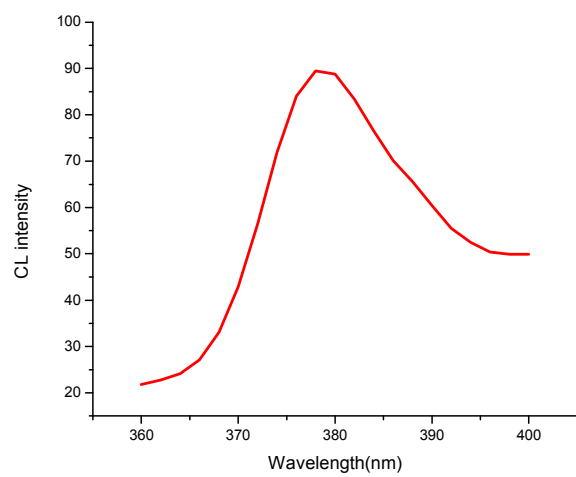
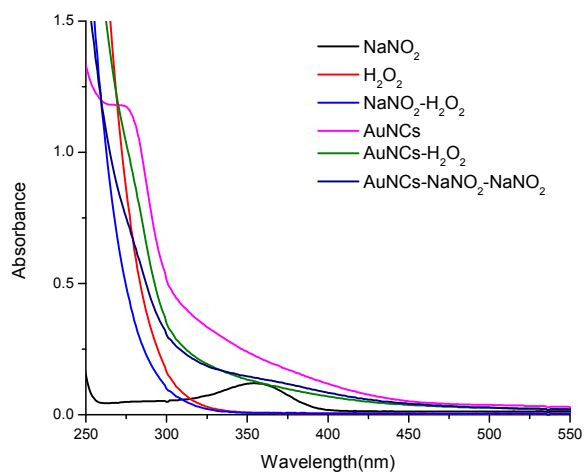


Fig.5



Scheme.1

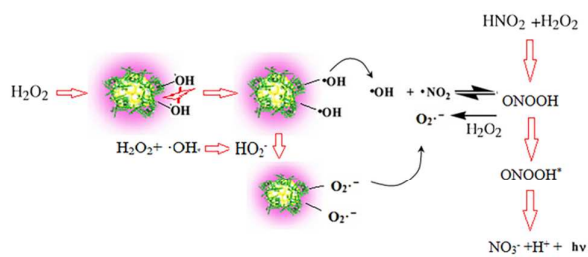


Fig.6

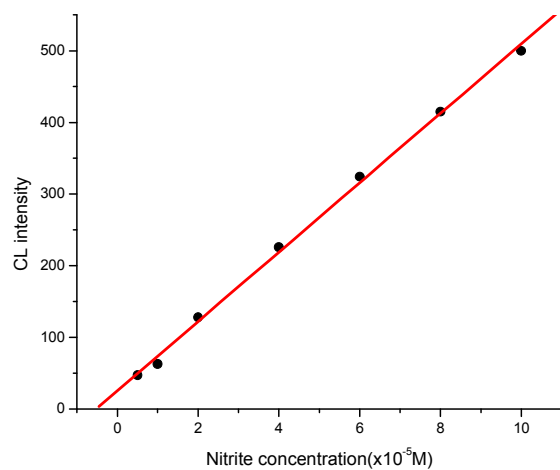
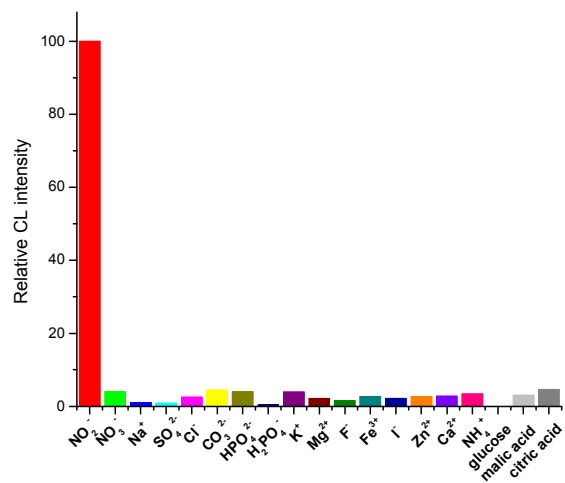
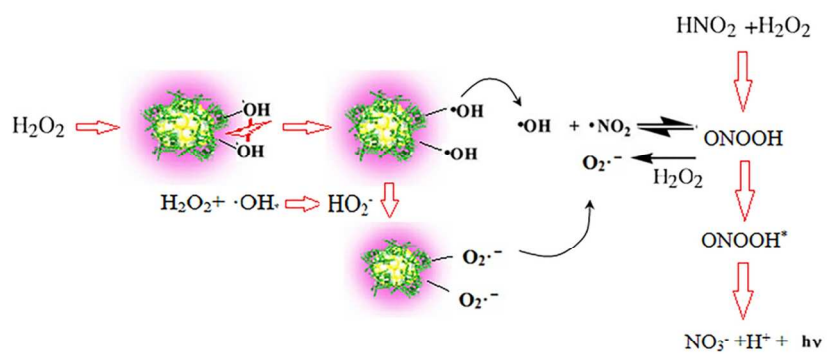


Fig.7





99x55mm (300 x 300 DPI)